



HAL
open science

Highly Oriented and Crystalline Films of a Phenyl-Substituted Polythiophene Prepared by Epitaxy: Structural Model and Influence of Molecular Weight

Amer Hamidi-Sakr, Daniel Schiefer, Sangeetha Covindarassou, Laure Biniek, Michael Sommer, Martin Brinkmann

► **To cite this version:**

Amer Hamidi-Sakr, Daniel Schiefer, Sangeetha Covindarassou, Laure Biniek, Michael Sommer, et al.. Highly Oriented and Crystalline Films of a Phenyl-Substituted Polythiophene Prepared by Epitaxy: Structural Model and Influence of Molecular Weight. *Macromolecules*, 2016, 49 (9), pp.3452-3462. 10.1021/acs.macromol.6b00495 . hal-02023083

HAL Id: hal-02023083

<https://hal.science/hal-02023083v1>

Submitted on 17 Dec 2021

HAL is a multi-disciplinary open access archive for the deposit and dissemination of scientific research documents, whether they are published or not. The documents may come from teaching and research institutions in France or abroad, or from public or private research centers.

L'archive ouverte pluridisciplinaire **HAL**, est destinée au dépôt et à la diffusion de documents scientifiques de niveau recherche, publiés ou non, émanant des établissements d'enseignement et de recherche français ou étrangers, des laboratoires publics ou privés.

Highly oriented and crystalline films of a phenyl-substituted polythiophene prepared by epitaxy : structural model and influence of molecular weight

Amer Hamidi-Sakr¹, Daniel Schiefer², Sangeetha Covindarassou¹, Laure Biniek¹, Michael Sommer^{2,3,4}, Martin Brinkmann¹

(1) Institut Charles Sadron, CNRS – Université de Strasbourg, 23 rue du loess, 67034 Strasbourg, France

(2) Institut für Makromolekulare Chemie, Universität Freiburg, Stefan-Meier-Straße 31, 79104 Freiburg, Germany

(3) Freiburger Materialforschungszentrum, Universität Freiburg, Stefan-Meier-Straße 21, 79104 Freiburg, Germany

(4) Freiburger Institut für Interaktive Materialien und Bioinspirierte Technologien, Georges-Köhler-Allee 105, 79110 Freiburg, Germany

Abstract

The large majority of semiconducting polymers based on poly(alkylthiophene)s with either linear or branched alkyl side chains are reported to π -stack in their crystalline phases. In regioregular poly(3-(2,5-dioctylphenyl)thiophene) (PDOPT), however, π - π interactions are absent due to the presence of the bulky 2,5-dioctylphenyl side groups. In this work, high levels of crystallinity and orientation are created in thin films of PDOPT aligned on substrates of naphthalene by slow directional epitaxial crystallization of the side chains. Depending on molecular weight, both edge-on and flat-on lamellar crystals are obtained. As for poly(3-hexylthiophene) (P3HT), electron microscopy imaging reveals a transition from extended to folded chain crystallization in PDOPT for $M_n \approx 12.7$ kDa. The high orientation and crystallinity result in high anisotropy in UV-vis absorption and photoluminescence with well defined vibronic structures. The single-crystal-like electron diffraction patterns are further used to refine a structural model of PDOPT ($a=29.09$ Å, $b=10.45$ Å, $c=7.72$ Å, $\alpha=\beta=\gamma=90^\circ$ and space group P21/c). Uniquely, crystalline PDOPT features perfectly planarized chains despite the absence of π -stacking between polythiophene backbones. The octyl side chains are interdigitated and crystallize in a dense subcell which is compared to that of other semiconducting polythiophenes e.g. form I poly(3-hexylthiophene) and poly(2,5-bis(3-dodecyl-2-yl)thieno[3,2-*b*]thiophene) to draw a trend between overall crystallinity and density of the side chain packing.

I. Introduction.

Conjugated polymers (CP) are of central importance in material science due to their unique optical and electronic properties that can be tuned by macromolecular engineering.^{1,2} Moreover, CPs are easy to process from solution to yield large thin film surfaces at low cost. However, small changes in the side chain substituents modify not only their processing from solution but also their supramolecular packing which controls the final electronic properties in thin films.³⁻⁸ The role and impact of side chain regioregularity and ordering is essential as it determines the degree of planarization of the conjugated backbone, and the extent of π -stacking upon crystallization.⁹ The disordering of side chains, e.g. upon a crystal to liquid crystal phase transition, can induce a twisting of the backbone, i.e. a rupture of conjugation that may result in a characteristic thermochromism.¹⁰ As a general rule, disorder in the π -stacking of semiconducting polymers such as P3HT and PBTTT determines the energetic disorder that controls charge mobility in layers of π -stacked chains.¹¹

At present, the influence of the side chain structure on charge transport is only poorly understood. One of the reasons might be that precise structural models of polythiophenes with different side chains are still relatively scarce. The inherent disorder of these semi-crystalline materials rests in the coexistence of crystalline and amorphous domains, and makes their structural refinement particularly challenging. Structure modeling based on grazing incidence X-ray diffraction (GIXD) or TEM data showed that alkyl side chains can be either interdigitated¹²⁻¹⁴ as in PBTTT and form II of P3HT, or not interdigitated as in form I P3HT.¹⁵ Recently, structural models of a P3HT oligomer and an analogue with branched 2-ethylhexyl side chains were investigated.¹⁶ Valuable structural data can be obtained from GIXD on non-oriented films and used to

elaborate some structural models of CPs. However, limited structural data can impede a reliable space group determination which is essential in the structural modeling of CPs as it defines the symmetry relation between monomeric units in a unit cell. Space group identification can only be done properly by using single-crystal-like diffraction patterns obtained from highly oriented or, more rarely, from CP single crystals.¹²

For all these reasons, it is essential to develop means to grow polymer films with well defined orientation and high crystallinity that yield single-crystal-like diffraction patterns suitable for structural refinement. Different strategies have been used to reach such characteristics in CP films. To cite but a few: epitaxy and directional epitaxial crystallization (DEC)^{17,18}, friction transfer¹⁹, controlled solvent vapor annealing (SVA)^{20,21} and high temperature rubbing.²²⁻²⁴ Controlled crystallization through self-seeding helped to refine the structure of form II of P3HT from well defined single crystal domains.¹² However, the preparation of such single crystals is usually tedious and therefore alternative approaches to prepare highly crystalline CP films are required. Epitaxial crystallization of CPs is an effective method to reach very high order and crystallinity as demonstrated recently.^{17,18,21,25-28} Directional epitaxial crystallization of P3HT and PFO was obtained with 1,3,5-trichlorobenzene (TCB) as a substrate.^{17,27} When using slow directional crystallization of TCB, it was possible to obtain very high orientation of both polymers over large surfaces.²⁶ Such highly oriented systems are ideally suited for structural refinement using electron diffraction.¹⁵ In epitaxied PFO films, almost single-crystal like diffraction patterns were used to establish a structural model of the α -polymorph.²⁷

Herein we report that epitaxy on naphthalene can lead to high degrees of orientation and crystallinity of a phenyl-substituted poly(thiophene), poly(3-(2,5-dioctylphenyl)thiophene) (PDOPT). PDOPT crystallizes well despite the presence of

bulky 2,5-dioctylphenyl side chains (see Figure 1.a).⁴ Sommer and coworkers reported on the first synthesis of highly regioregular PDOPT and the growth of micron-sized spherulites using isothermal crystallization, for which a high degree of regioregularity was crucial.^{29,30}

In the present contribution, thin films of highly oriented and crystalline PDOPT with single-crystal-like diffraction patterns are prepared by slow directional epitaxial crystallization on naphthalene for different samples with molecular weights $M_{n,SEC}$ = 6-38 kDa. Liquid naphthalene is a solvent for PDOPT but becomes a substrate for epitaxy of PDOPT in its crystalline form. The influence of M_n on the film morphology has been investigated by TEM and electron diffraction. From single crystal-like diffraction patterns a structural model is determined which shows that the polythiophene backbone is highly planar despite the absence of π - π interactions. Polarized UV-vis and fluorescence measurements are also used to investigate the impact of orientation and crystallinity on the thin film optical properties.

II. Experimental section

a) Materials

Naphthalene with 99% purity was purchased from Sigma Aldrich. The synthesis of the PDOPT samples proceeds via Kumada catalyst transfer polycondensation and is described in detail elsewhere.²⁹ The study of the molecular weight of PDOPT on its structural characteristics was made on a set of six polymer batches with M_n in the range 6.2-37.6 kDa. The relevant macromolecular parameters were obtained by size exclusion chromatography (SEC) and are summarized in Table 1 (Figure S1).

Table 1. Macromolecular data of the PDOPT samples.

M_n^a [kDa]	M_w^a [kDa]	PDI ^a	DP _n
6.2	6.7	1.08	16.2
7.8	8.7	1.12	20.4
9.2	12.1	1.31	24.1
12.7	19.8	1.56	33.2
21.0	36.1	1.72	55.0
37.6	74.4	1.97	98.4

^a Polydispersity (PDI) index and degree of polymerization (DP_n) obtained via SEC in THF with polystyrene standard.

b) Thin film preparation

Epitaxial thin films are prepared by using a modified directional epitaxial crystallization method. In brief, it consists of using a crystallizable solvent (naphthalene) playing successively the role of (i) the solvent for PDOPT in its liquid form and (ii) once crystallized, the substrate for the epitaxial crystallization of the polymer. The process implies several steps described elsewhere.³¹ In brief, a solution of PDOPT (1 mg)/naphthalene (200mg) is spread between two clean glass slides by capillary forces. One glass substrate is coated with an oriented film of PTFE to guide the in-plane crystallization of naphthalene. The sample is moved in a home-made system allowing for a local zone melting of naphthalene at a setting temperature of 113°C and a translation speed of 20 μm/s (see Figure 1.b). After directional crystallization of naphthalene, the PDOPT films are orange, indicating that they are non-crystalline, presumably because the PDOPT film is still swollen with naphthalene. The films are placed in a freezer at -6°C for one minute to lower the high vapor pressure of naphthalene and induce crystallization of PDOPT, indicated by a color change to violet-purple. The films remain crystalline at room temperature. Naphthalene is removed by

sublimation under a primary vacuum , leaving a highly oriented film of PDOPT on the glass substrate.

c) TEM analysis

Oriented areas are selected by optical microscopy (Leica DMR-X microscope) for TEM analysis. A thin carbon film is evaporated onto the PDOPT films using an Auto 306 evaporator (Edwards). The sample is removed from the glass substrate by floating the films on a 5 wt% aqueous HF solution and recovered on copper grids. TEM is performed in bright field, high resolution and diffraction modes using a CM12 Philips microscope equipped with a MVIII (Soft Imaging System) CCD camera. Specific conditions for low dose diffraction are given elsewhere.^{32,33} Calibration of reticular distances is performed by using an oriented poly(tetrafluoroethylene) thin film.

Molecular modelling is performed on a Silicon Graphic station using the Cerius2 program (Accelrys). A trial-and-error procedure was used to refine the crystal structure of PDOPT, following the methodology used previously for P3HT³⁴, PF8³⁵ and PCPDTBT³⁶ and conjugated co-oligomers³⁷. For each step of the trial-and-error method, the molecular geometry is optimized using the “clean” procedure of the Cerius2 3.0 Program (additional information on this procedure is available in the User’s guide on Modeling Environment). For the single crystal diffraction calculations, a crystal thickness of 30 nm was used. Energy minimization was performed using the minimizer module of the Cerius2 program and the United Force Field UFF1.1.

d) Polarized UV-vis and fluorescence spectroscopy

Polarized UV-vis absorption spectroscopy was performed using a Varian Carry 5000 UV-VIS-NIR spectrometer with polarized incident light. The photoluminescence of PDOPT films was measured with a Jobin – Yvon FluoroMax 4 spectrofluorimeter with a slit width of 3 nm for both the excitation and the detection. Excitation was performed at a wavelength of 540 nm.

III. Results and discussion

1. Evidence for orientation (POM, UV-vis spectroscopy)

Directional epitaxial crystallization is an effective method to achieve high orientation and alignment of conjugated semiconducting polymers. 1,3,5-trichlorobenzene in its liquid form ($T > 63^\circ\text{C}$) is a perfect solvent for P3HT and PFO whereas when it crystallizes, it becomes the substrate for the epitaxial growth of the polymer. The effectivity of a crystallizable solvent such as TCB is related to the possibility for an epitaxial crystallization i.e. a registry between the substrate and the polymer crystal unit cell parameters in at least one direction (1D epitaxy).¹⁷ For P3HT, 1D epitaxy was evidenced on TCB substrates. Attempts to use TCB failed in the case of PDOPT, but naphthalene (NA) proved to be very efficient to induce orientation of the polymer. As opposed to TCB, NA is a non chlorinated solvent with low melting temperature (80.5°C) and sublimes easily under primary vacuum at room temperature. Large surfaces of oriented films are produced in a home made zone melting system as shown in Figure 1.b. The growth front of NA moves at $20 \mu\text{m/s}$ which yields NA crystals elongated in the direction of the \mathbf{a}_{NA} axis with a dominant (0 0 1) contact plane (monoclinic crystal structure : $a = 8.09\text{\AA}$, $b = 5.95\text{\AA}$, $c = 8.65\text{\AA}$, $\beta = 124.4^\circ$).³⁸

Figure 1 shows the polarized optical microscopy images of two highly oriented PDOPT films of different M_n s grown by slow directional epitaxial crystallization. Both

PDOPT samples exhibit remarkable orientation as illustrated by the color change from deep purple/red to almost colorless when the light polarization (Pol) changes from parallel to perpendicular with respect to the chain direction. The alignment of PDOPT chains along the fast growth direction of naphthalene is epitaxial as demonstrated by TEM (vide infra).

Further evidence for the high alignment is supported by polarized UV-Vis and photoluminescence (PL). Figure 2 illustrates the high anisotropy observed in absorption and PL for PDOPT films with 6 kDa and 21 kDa oriented by slow-DEC on NA, resulting in dichroic ratios in the range 8-10 for absorption and PL. These values are higher than those observed by micro-photoluminescence on spherulites, presumably due to a higher level of in-plane orientation of crystalline domains in the epitaxied films whereas a splay of the lamellar orientations is common in spherulites.³⁰

Most interesting is the well defined vibronic structure in the PL of all PDOPT films. The PL spectra are well modeled with a single Franck-Condon progression (see Figure S2). The obtained Huang-Rhys factor S in the range 0.69 – 0.77 indicate a small electron-phonon coupling.³⁹ Fitting with a single F-C progression suggests that a single emitting species is involved in PDOPT films. In contrast, thin films of P3HT cooled from the melt have two H-type aggregate emitting species.⁴⁰ This difference might be related to the absence of π - π stacking in PDOPT for which inter-chain excitonic coupling might be very small as opposed to P3HT. However, the UV-vis absorption spectrum for Pol // C_{PDOPT} (see Figure 2) is very similar to that of P3HT and cannot be accounted for by a single vibronic progression : it contains the signature of excitonic coupling in the crystal. From previous analyses of the vibronic structure in crystalline P3HT, the predominance of the 0-0 vibronic component over the 0-1, is indicative of highly planarized chain segments in the crystalline domains. This is accordingly also the case for PDOPT as

demonstrated further by TEM. The absorption spectra for $\text{Pol} \perp \text{C}_{\text{PDOPT}}$ are less structured and in general blue-shifted relative to $\text{Pol} // \text{C}_{\text{PDOPT}}$. This results from the semi-crystalline lamellar morphology of the PDOPT films. For $\text{Pol} \perp \text{C}_{\text{PDOPT}}$, the UV-vis absorption spectrum is dominated by the non structured absorption of amorphous, non-oriented PDOPT domains as also observed previously in oriented PBTTT and P3HT films.^{22,24} This result points to the semi-crystalline structure of PDOPT, that is again further evidenced by TEM.

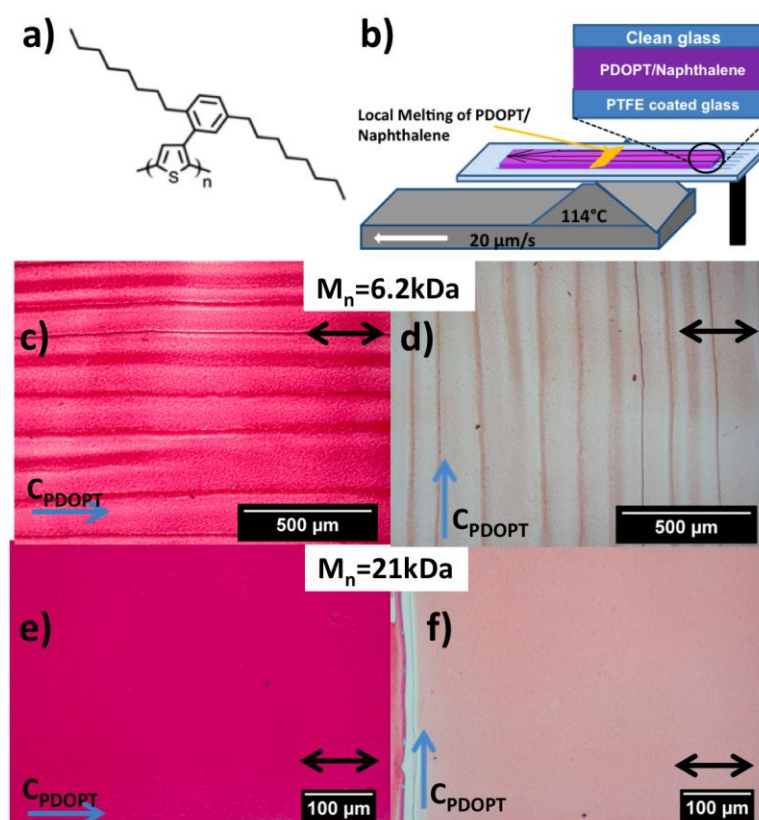


Figure 1. (a) Chemical formula of PDOPT. (b) Setup used for the growth of oriented PDOPT films by directional epitaxial crystallization. It consists of a heated pyramidal base kept at a setting temperature of 113°C. Upon moving the PDOPT/naphthalene blend between two glass substrates, local melting causes the crystallization front of naphthalene to grow steadily at 20 $\mu\text{m/s}$. (c) – (f) POM images of highly oriented PDOPT films with $M_n = 6.2$ and 21 kDa. The direction of the PDOPT chains is indicated by a blue

arrow whereas the direction of the polarization of the incident light is indicated by a double arrow.

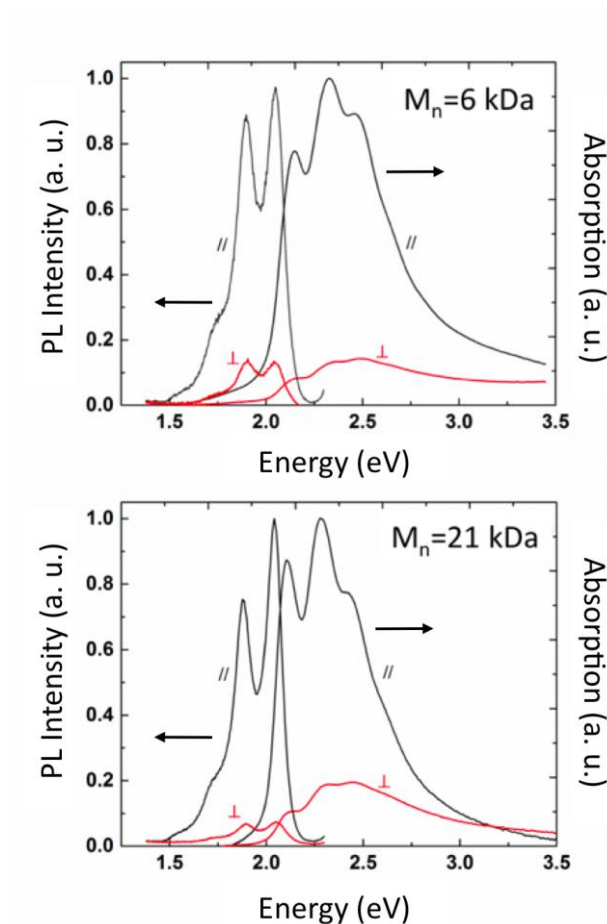


Figure 2. Comparison of the polarized absorption and photoluminescence of highly oriented and crystalline PDOPT films prepared by slow DEC on naphthalene for two different molecular weights. All curves in black (resp. red) correspond to the absorption measured with incident light polarization parallel (resp. perpendicular) to the chain direction and the emission polarized parallel (resp. perpendicular) to the chain direction. The spectra obtained for Pol/cPDOPT are normalized to 1. For the photoluminescence, the excitation light ($\lambda = 540$ nm) was polarized parallel to the chain direction.

The structure and morphology of the epitaxied PDOPT films was examined by TEM. Figure 3 compares the bright field and diffraction patterns of the PDOPT films ($M_n=21$ kDa) obtained by doctor-blading from *ortho*-dichlorobenzene (ODCB) (a), isothermal crystallization at 100°C for 24 hrs (b) and epitaxy on NA (c). All samples consist of lamellar edge-on crystals but the lamellar periodicity depends on the preparation conditions: 16 nm for doctor bladed films, 20 nm for isothermal crystallization at 100°C and 27 nm for the epitaxied films. The in-plane dimensions of crystalline lamellae and their relative organization are also a function of the preparation conditions. The smallest lamellar periods are observed for the doctor-bladed films (Figure 3a). In this case, there is no control of the relative orientation between crystalline lamellae contrary to the isothermally crystallized samples that show spherulites in POM (see Figure 3.b) whose birefringence reflects the ordered arrangement of lamellae. Successive lamellae in PDOPT spherulites show a characteristic splay that results from the loss of local relative in-plane orientation between successive lamellae when moving from the center to the periphery of the spherulites. In strong contrast, perfect in-plane orientation of the PDOPT lamellae is observed in the epitaxied films over several hundreds of microns, due to the alignment induced by the naphthalene substrate. The ED patterns of all three PDOPT samples show reflections with identical reticular distances indicating that the same polymorph is obtained in all cases, independently of the preparation method. Structural similarities are also manifested in very similar UV-vis absorption spectra obtained for all three samples (Figure S3). Only a stronger contribution of the 0-2 vibronic component is observed for the epitaxied film.

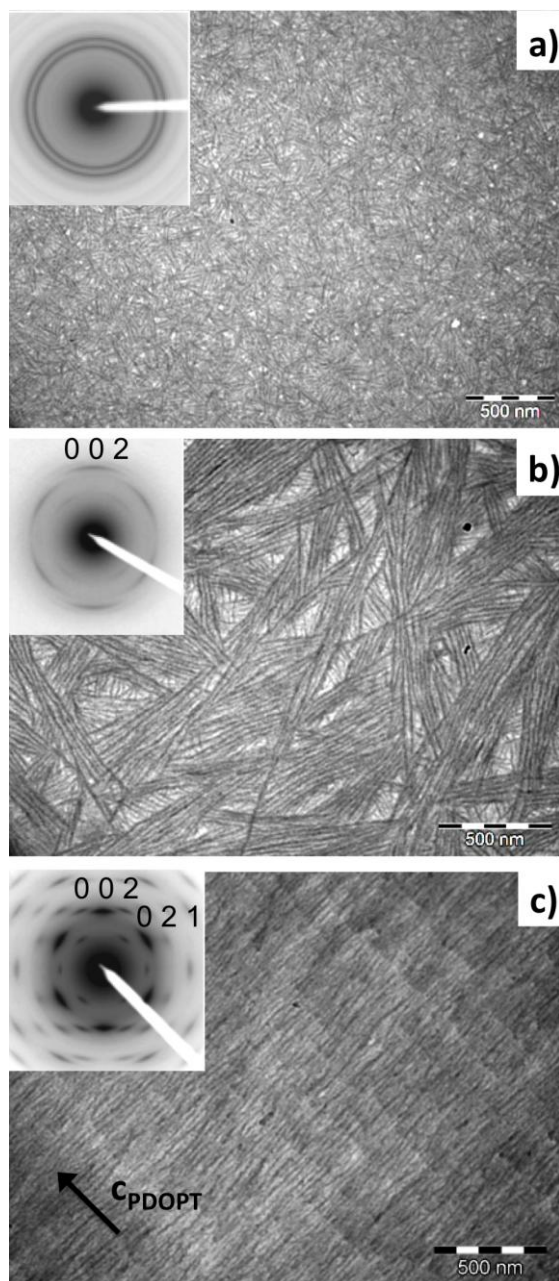


Figure 3. Comparison of the bright field TEM images and corresponding diffraction patterns of the PDOPT films ($M_n = 21$ kDa) obtained by doctor-blading from ODCB (a), isothermal crystallization at 100°C for 24 hrs (b) and epitaxy on NA (c). The arrow in (c) indicates the in-plane direction of the PDOPT chains.

2. Effect of molecular weight on structure, morphology and optical properties

a) Lamellar periodicity

The morphology of the epitaxied films was observed in Bright field TEM (Figure 4a-d). Figure F.d features the evolution of the total lamellar period L as a function of M_n .¹⁷ The regular lamellar structure is characteristic of semi-crystalline polymers and is similar to that observed previously for P3HT films oriented on TCB.¹⁷ The contrast in the BF images is between amorphous interlamellar zones and crystalline lamellae of PDOPT.¹⁷ In all PDOPT films, highly oriented lamellae are observed with edge-on orientation. PDOPT lamellae with very uniform thickness are formed for $M_n=7.8$ kDa whereas for $M_n \geq 21$ kDa strong fluctuations in the lamellar thickness result in peak broadening in the fast Fourier transforms (FFT) of the BF images. Molecular weight dispersity might be responsible for this behaviour, at least in part (see Table 1).²⁹ The lamellar periods L obtained from FFTs of the TEM images reveal a clear trend with M_n , shown in Figure 3.e. For $M_n \leq 12.7$ kDa, L scales with M_n whereas for $M_n \geq 21$ kDa, L saturates at ~ 29 nm. This trend is similar to that observed for epitaxied P3HT films (see Figure 4.e). It indicates that PDOPT chains with $M_n \leq 12.7$ kDa tend to crystallize with extended chains whereas for $M_n \geq 21$ kDa, chain folding comes into play.^{18,41} Such a transition in the crystallization mode is characteristic of semi-crystalline polymers. The comparison with P3HT is further instructive in that the L values at saturation for the folded chain systems are almost identical and close to 28-29 nm for both P3HT and PDOPT. This similarity suggests that the upper L of 28-29 nm observed in folded-chains of polythiophenes is only marginally determined by the nature of the side chains : it is therefore a characteristic of the polythiophene chain folding, irrespective of the side chain.

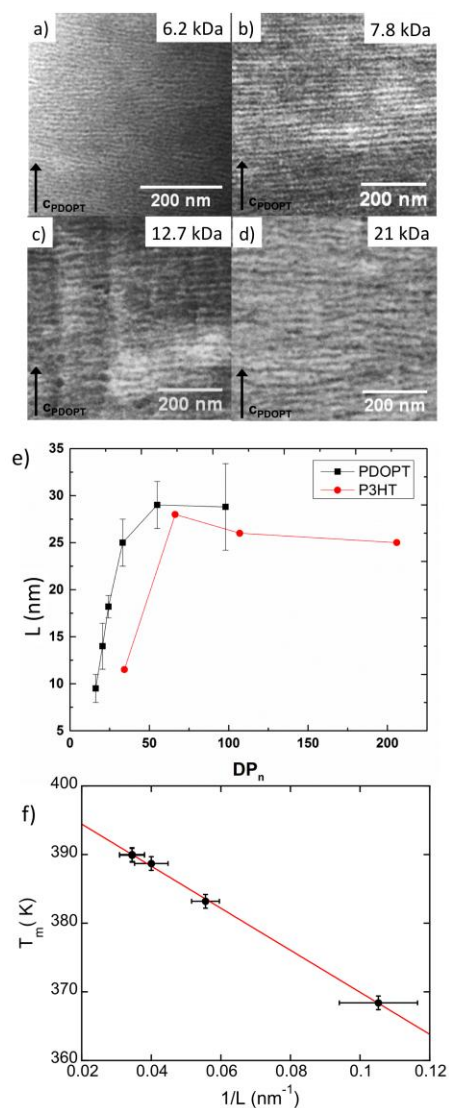


Figure 4. a) – d) : Evolution of the semicrystalline lamellar morphology in oriented PDOPT as a function of molecular weight (M_n) as observed in bright field TEM. e) Evolution of the average lamellar periodicity as extracted from the fast Fourier Transform of the TEM BF images. As a comparison, the lamellar periodicities L_p observed in a previous study on epitaxied P3HT are also shown as a function of the degree of polymerization DP_n .¹⁸ f) Evolution of the melting temperature T_m measured by DSC as a function of the total lamellar periods L measured by TEM for PDOPT samples with different molecular weights. The full line is the result of a linear fit following a Gibbs-Thomson analysis (see text).

A Gibbs-Thomson analysis was attempted using the melting temperatures determined by DSC²⁹ and the lamellar periods measured by TEM for PDOPT samples of different M_n . The correlation between the melting temperature T_m and the lamellar period L of polymer crystals follows usually the equation⁴²:

$$T_m = T_m^0 \left[1 - \frac{2\sigma_e}{L \Delta H_m} \right] \quad (1)$$

where T_m^0 is the equilibrium melting temperature of a PDOPT crystal with infinite size, ΔH_m is the equilibrium enthalpy of melting for a crystal of infinite size and σ_e is the crystal surface free energy. As seen in Figure 4.f, a very good agreement is obtained when the experimental values of T_m measured by DSC are plotted versus $1/L$, yielding a value $T_m^0 = 127.6^\circ\text{C} \pm 1^\circ\text{C}$. It must be stressed that this relation seems to hold true even if the melting temperatures are measured for PDOPT powders and not epitaxied PDOPT films, suggesting that the lamellar periods observed in the powders of the different PDOPT samples should be comparable to those observed in the films grown by epitaxy. At present, the value of ΔH_m for a 100% crystalline PDOPT sample remains unknown, making the extraction of σ_e from equation (1) difficult. Additional efforts are currently in progress to determine ΔH_m of 100% crystalline PDOPT.

b) Electron diffraction

In our previous study on the impact of M_n on the structure and morphology of P3HT films prepared by slow DEC, the samples of lower M_n showed the most well defined ED patterns, indicating that crystallinity was most pronounced for shorter chains. Figure 5 shows the evolution of the ED patterns of oriented PDOPT films with increasing M_n . All the ED patterns show the same characteristic reflections, indicating

that a single polymorph with one dominant contact plane is formed on naphthalene. This same polymorph is present in films prepared by doctor-blading and isothermal crystallization. The main reflections are indexed with an orthorhombic unit cell ($a=29.1\text{\AA}$, $b=10.5\text{\AA}$ and $c=7.72\text{\AA}$, $\alpha=\beta=\gamma=90^\circ$). All ED patterns correspond to the $[1\ 0\ 0]$ zone with very intense $0\ 0\ \pm 2$, $0\ \pm 2\ 1$ and $0\ 2\ \pm 1$ reflections forming a hexagonal-like pattern ($d_{002} = 3.86\text{\AA}$ and $d_{021} = 4.33\text{\AA}$). As shown hereafter, this pseudo-hexagonal pattern is similar to that of polyethylene single crystals and is a fingerprint of the regular packing of the *n*-octyl side chains.⁴³ The pattern dominates the ED of PDOPT films because the orientation of crystalline lamellae is such that the electron beam is parallel to the *n*-octyl side chain axis, with the polythiophene backbones lying in the plane of the substrate (see Figure 5.e). This contact plane is also observed in the doctor bladed films and the spherulites after isothermal crystallization on SiO₂ substrate.

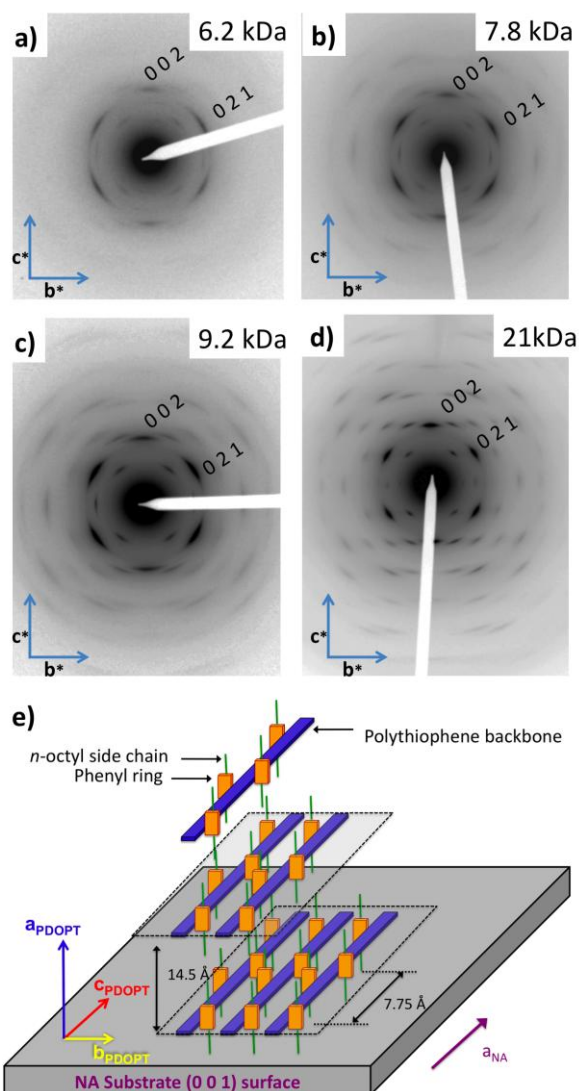


Figure 5. Comparison of the ED patterns for oriented films of PDOPT prepared by epitaxy on naphthalene for different molecular weights (a)-(d). All patterns correspond to the [1 0 0] zone i.e. the incident electron beam is parallel to the direction of the n -octyl side chains of PDOPT. Note the progressive improvement in the structural perfection of the PDOPT crystals as M_n increases. (e) Schematic illustration of the dominant orientation of the PDOPT crystals on the naphthalene substrate.

With increasing M_n , the presence of higher order reflections with d_{hkl} up to 1.3 \AA^{-1} indicates a progressive improvement of crystalline order. This trend is a consequence of

the increased total lamellar period. Larger values of L imply larger crystalline domains in the chain axis (c axis) direction, hence, improved diffraction of crystallites. PDOPT behaves therefore differently from P3HT whose crystallinity in epitaxied films was observed to decrease with increasing M_n .¹⁸ This comparison points at the beneficial role of the 2,5-dioctylphenyl groups on the crystallization of higher molecular weight PDOPT.

For PDOPT with $M_n = 6.2$ kDa, the majority of crystals have a (1 0 0) contact plane on naphthalene i.e. like other molecular weights. However in some parts of the samples (essentially the thinnest parts of the films), additional and different ED patterns corresponding to a minority fraction of PDOPT crystals with two different contact planes on naphthalene are identified. Figure 6, features these two additional and characteristic diffraction patterns and the corresponding defocused ED patterns in proper relative orientation to the ED. The two additional ED patterns can be indexed by using the same structure as for the dominant orientation. They correspond to i) flat-on lamellar crystals with standing PDOPT chains ([0 0 1] zone) and to ii) crystals of PDOPT with n -octyl side chains flat-on the substrate plane ([0 1 0] zone) (see the schematic illustrations in Figure 6e and 6f). In both cases, the lamellae show up as light grey areas in the morphology image (defocused ED) in contrast to the darker i.e. thicker edge-on lamellae. For flat-on crystals, the quantized changes in grey levels reveal multilamellar morphologies. The presence of the PDOPT crystals with standing chains for the 6.2kDa sample reminds the case of P3HT films epitaxied on TCB.^{18,26} Indeed, it has been shown that P3HT crystals with standing chains are also observed for epitaxied films with low molecular weight (7.3 kDa).¹⁸ In the case of P3HT, it was suggested that a mechanism of homoepitaxy could explain the growth of flat-on lamellar crystals on edge-on crystals. Such a mechanism is only possible for polymers crystallizing with extended chains i.e.

when the surface of the lamellar crystals is not made of folded i.e. disordered chains. In other words, the presence of PDOPT crystals with standing chain for 6.2 kDa is a further evidence for extended chain crystallization for such low M_n .

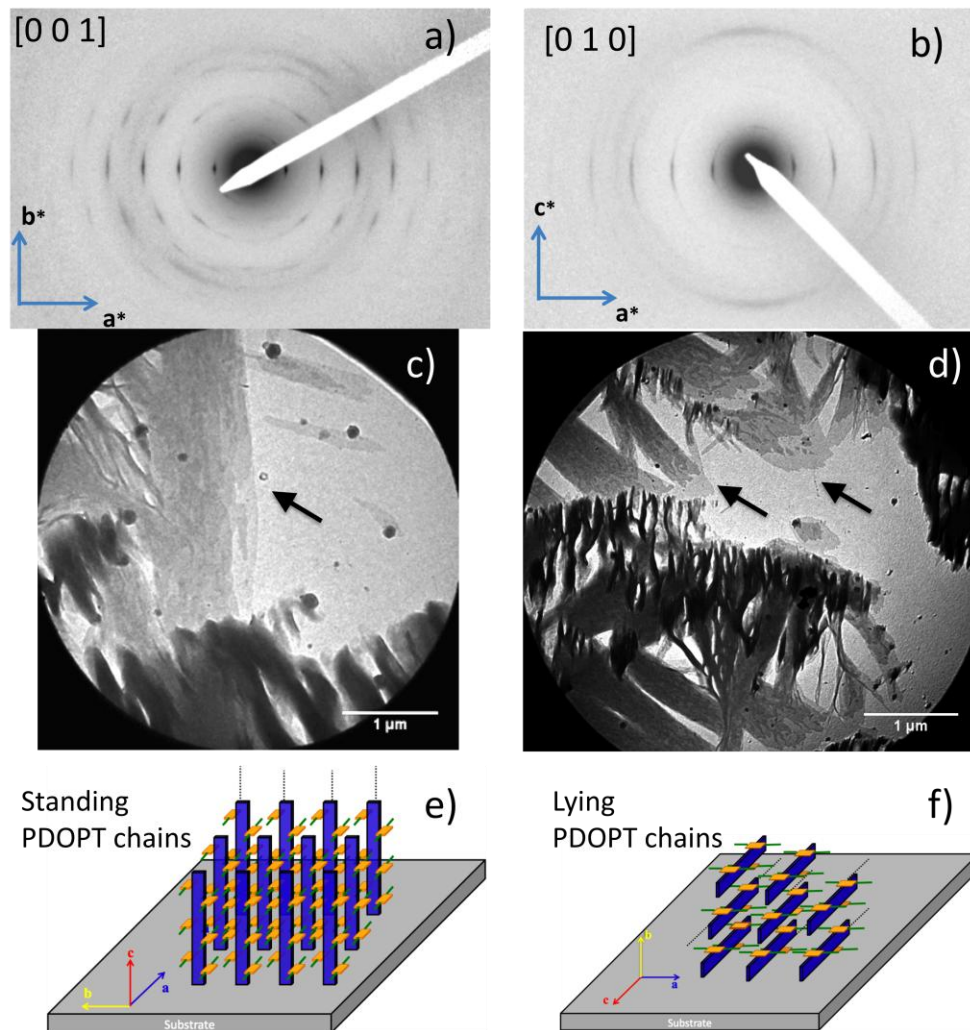


Figure 6. Selected area diffraction patterns and associated morphologies in 6.2kDa PDOPT films observed for a minority of PDOPT lamellar crystals on naphthalene. The corresponding defocused diffraction patterns feature the morphology of the diffracting areas for the [0 0 1] (c) and the [0 1 0] zone (d). These orientations correspond to the [0 0 1] i.e. standing chains (a) and to the [0 1 0] zone (b). The schematic illustrations in (e) and (f) show the orientation of the crystalline domains with respect to the substrate

plane for the [0 0 1] and [0 1 0] zones, respectively. In (c) and (d), the arrows point at flat-on PDOPT lamella crystals.

c) Epitaxy

The relative orientation of PDOPT on NA corresponds to : $(1\ 0\ 0)_{\text{PDOPT}} // (0\ 0\ 1)_{\text{NA}}$ and $\mathbf{c}_{\text{PDOPT}} // \mathbf{a}_{\text{NA}}$ (the growth direction of naphthalene using a Bridgman type of growth corresponds to the $(1\ 0\ 0)_{\text{NA}}$ direction³⁸). To determine if epitaxy is a possible mechanism for the observed orientation of PDOPT chains, it is necessary to compare the unit cell parameters of the PDOPT overlayer and the naphthalene substrate. The possibility for epitaxy is usually determined by the mismatch factors between the unit cell parameters of the overlayer and the substrate.⁴⁴ These parameters can be evaluated for PDOPT on NA :

- along the chain direction : $|\mathbf{c}_{\text{PDOPT}} - \mathbf{a}_{\text{NA}}|/\mathbf{c}_{\text{PDOPT}} \approx 4\ \%$
- perpendicular to the chain direction : $|\mathbf{b}_{\text{PDOPT}} - 2\mathbf{b}_{\text{NA}}|/\mathbf{b}_{\text{PDOPT}} \approx 12\%$.

Only the mismatch parameter along the chain direction of PDOPT is below 10% which is commonly considered as the upper limit for epitaxial growth. Accordingly, it seems that the epitaxy of PDOPT on NA involves essentially a 1D epitaxial orientation mechanism. This situation is close to that observed for P3HT epitaxy on TCB for which $\mathbf{c}_{\text{P3HT}}//\mathbf{c}_{\text{TCB}}$ with a mismatch $|\mathbf{c}_{\text{P3HT}} - 2*\mathbf{c}_{\text{TCB}}|/\mathbf{c}_{\text{P3HT}} \approx 2.5\%$.¹⁷ As an illustration, Figure 7 features the section profile of the PDOPT/NA interface. It shows that ordering of the *n*-octyl side chains by 2D epitaxy on naphthalene is clearly the driving force for the alignment of PDOPT since the polythiophene backbones are approx. 10 Å away from the NA contact plane.

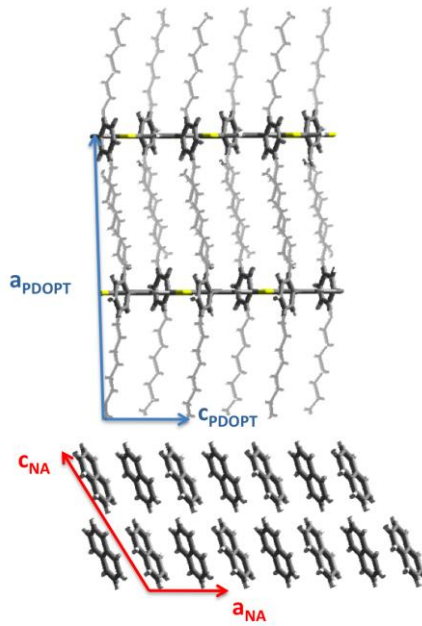


Figure 7. Structural model showing the section profile of the $(1\ 0\ 0)_{\text{PDOPT}}/(0\ 0\ 1)_{\text{NA}}$ interface. Note the epitaxial growth condition $c_{\text{PDOPT}}//a_{\text{NA}}$ with $|c_{\text{PDOPT}} - a_{\text{NA}}|/c_{\text{PDOPT}} \approx 4\%$ indicating that orientation of PDOPT chains is due to the 1D epitaxial orientation of the *n*-octyl side chains on NA.

3. Structural model of PDOPT

The control of orientation and crystallinity in epitaxied films of PDOPT opens the route to a structural refinement of this polymer. The trial-and-error approach followed herein is similar to that used in our previous studies on form I P3HT¹⁵, PFO²⁷ and PCPDTBT/F-PCPDTBT.²¹ First, the different diffraction patterns obtained for different zone axes are used to determine the selection rules of the observed reflections. The 35 – 40 independent reflections obtained from the collected ED patterns are indexed using an orthorhombic unit cell with parameters $a=29.1\text{\AA}$, $b=10.5\text{\AA}$ and $c=7.72\text{\AA}$, $\alpha=\beta=\gamma=90^\circ$, i.e. unit cell dimensions essentially similar to those proposed by Aasmundveit et al. on the basis of powder diffraction data.⁴ In their case, the absence of diffraction data along the

chain direction hampered the space group identification. This uncertainty is presently alleviated. The following selection rules are identified and point to the P21/c space group⁴⁵:

$$(h\ 0\ 0) \text{ with } h=2n$$

$$(k\ 0\ 0) \text{ with } k=2n$$

$$(0\ 0\ l) \text{ with } l=2n$$

$$\text{and } (h\ k\ 0) \text{ with } h+k=2n$$

Accordingly, the unit cell contains four monomer units related by the symmetry conditions (x, y, z) , $(-x+1/2, -y+1/2, z+1/2)$, $(-x, -y, -z)$ and $(x+1/2, y+1/2, -z+1/2)$. As expected for a regioregular PDOPT chain, successive monomers in a chain are related by a 21 screw axis.

The structural refinement was performed in two steps. First, the best agreement between calculated and experimental ED pattern was sought by a simple trial-and-error approach. In a second step the lattice energy of this unit cell was minimized. The experimental and the calculated ED patterns for the $[1\ 0\ 0]$ and the $[0\ 0\ 1]$ zones before and after energy minimization are given in Figure 8. The corresponding projections of the structural models are shown in Figure 9. After energy minimization, a final stable structure that is very similar to the initial model (see Figure 9) was obtained. The calculated ED patterns for both models are similar, indicating that the trial-and-error approach leads to structural models that are relatively accurate first order solutions even though the exact packing of the *n*-octyl side chains could only be obtained after energy minimization. Closer inspection of the calculated ED patterns show some differences because the energy minimization results in a small reorientation of the *n*-octyl side chains in the unit cell. In the initial model obtained by trial-and-error approach, *n*-octyl side chains are set parallel to the **a** axis, as in the model of

Aasmundveit et al.⁴ However, in this structure, the packing of *n*-octyl side chains was not optimized. Only for the second model i.e. after energy minimization is a satisfactory packing of the side chains obtained at the expense of a small tilt of the *n*-octyl side chains to the **a** axis. The optimized model yields a substantial improvement of the [0 0 1] zone, in particular the low intensity of the $\pm 1\ 1\ 0$ reflection is well reproduced while in the initial model it was strongly overestimated. *A contrario*, the strong $0\ \pm 1\ 2$ reflection is lost after energy minimization in the calculated [1 0 0] zone.

The refined model of PDOPT is close to that proposed earlier by Aasmundveit et al.⁴ The major improvement lies in the clearcut determination of the space group given the highly defined ED patterns obtained for the [1 0 0] and [0 0 1] zones. In particular, all other symmetry relations between monomers in the unit cell proposed as alternative models by Aasmundveit et al. can be discarded because they lead to some unobserved reflections in the diffraction patterns, e.g. $0\ 1\ 0$ and $0\ 0\ 1$ reflections.⁴ PDOPT chains have a perfectly planarized backbone, in agreement with the conclusions drawn from optical properties. Contrary to most semi-conducting polymers such as P3HT or PBTTT, the backbone planarization of PDOPT is not enforced by π - π stacking. The 2,5-dioctylphenyl side groups are oriented in a plane perpendicular to the chain axis and the *n*-octyl side chains form a strongly interdigitated sublattice. The plane of the phenyls is almost perpendicular to the plane of the polythiophene backbone. Successive phenyl groups along the **b** axis are however not in a situation of favorable π - π stacking. The top view of the *n*-octyl side chain sublattice is shown in Figure 10.g, its parameters are $a_0 = b_{\text{PDOPT}} = 10.5\text{\AA}$ and $b_0 = c_{\text{PDOPT}} = 7.72\text{\AA}$. Such a sublattice can be compared to that of regular polymethylenes e.g. the **M**, **T** and **O** sublattices.⁴³ As a matter of fact, the *n*-octyl sublattice in PDOPT is twice a classical **O** subcell with slightly larger unit cell parameters (typically $a_0 = 4.96\text{\AA}$ and $b_0 = 7.40\text{\AA}$ for **O** subcell).⁴³ As a consequence, the average

molecular area per *n*-octyl stem (20.17 \AA^2) is close to that observed for the classical **O** polymethylene subcell (18.4 \AA^2).⁴³ The doubling of the subcell area is due to the fact that two *n*-octyl side chains are linked to the phenyl group as illustrated in Figure 10.

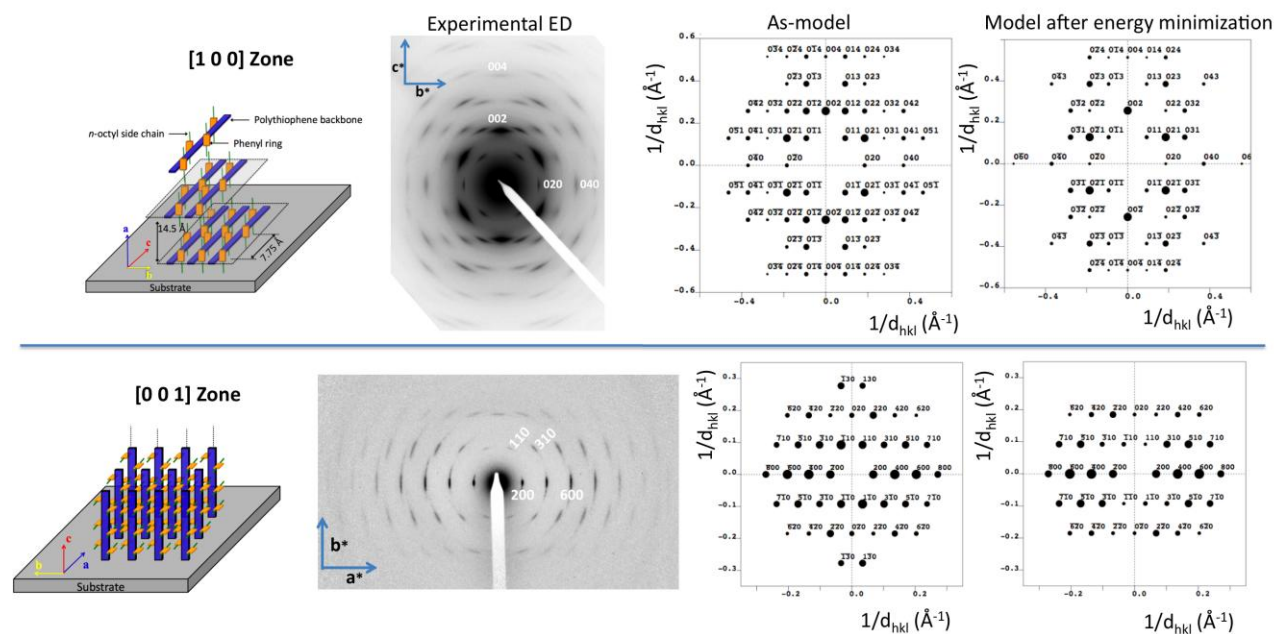


Figure 8. Comparison of the experimental electron diffraction patterns of highly oriented PDOPT films (6 kDa) grown by slow-DEC on naphthalene corresponding to the [1 0 0] and the [0 0 1] zones with the calculated ED patterns obtained for the structural model obtained by trial-and-error (as-model) and after energy minimization.

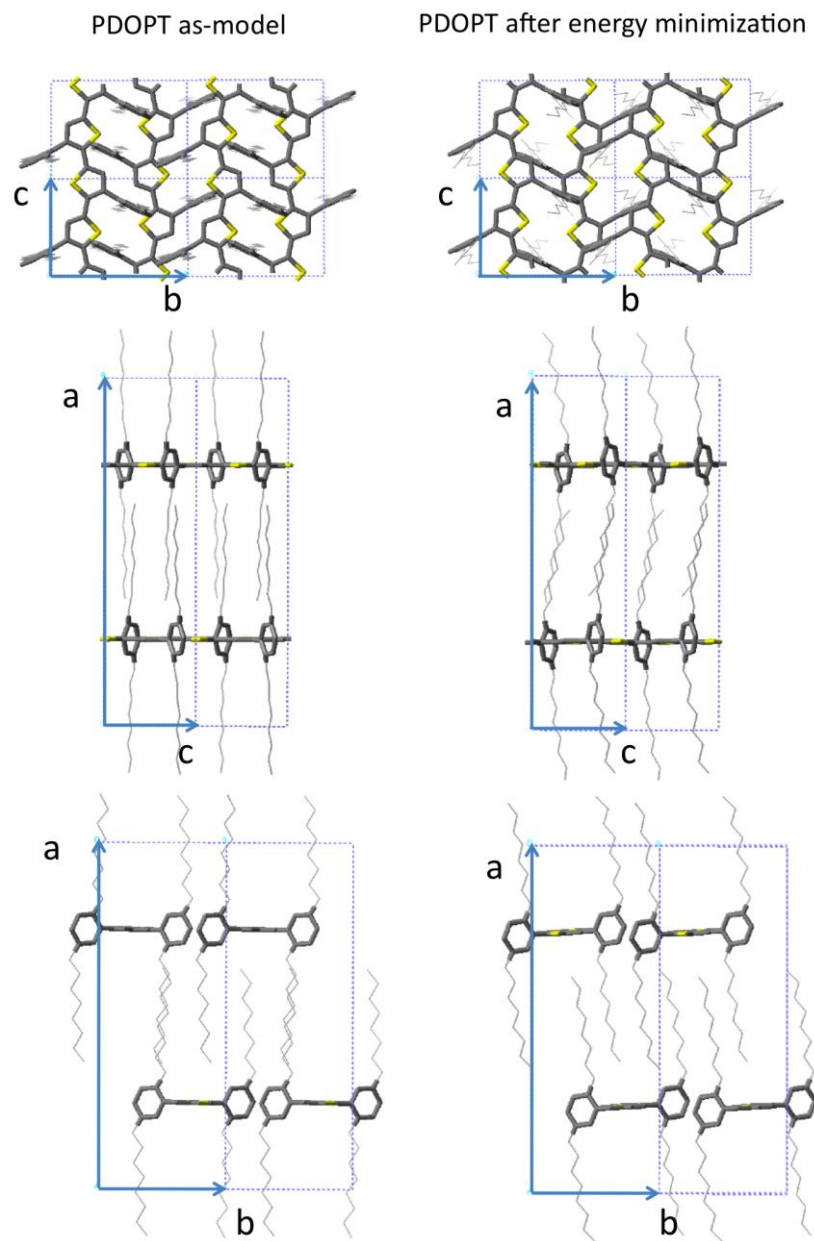


Figure 9. Projections of the refined structure of PDOPT along the **c**, **b** and **a** unit cell axes for the model obtained by trial-and-error and after energy minimization.

IV. Discussion

At present, only a limited number of structures of CPs have been determined precisely by using X-ray diffraction, electron diffraction or molecular mechanics methods.^{13,15} However, to correlate properties such as charge transport to the packing of the chains in a crystal, it is important to determine the type of sublattice formed by the alkyl side chains, especially because the side chain ordering/disordering can impact the planarization of the conjugated backbone and hence electronic properties of the CPs. In this perspective, it is instructive to compare the sublattices formed by alkyl side chains in a number of poly(thiophene)s for which structural models have been recently proposed e.g. PDOPT, form I P3HT and C12-PBTTT. Figure 10 compares the projections of the polymethylene subcells along the alkyl chain direction for P3HT, PDOPT and C12-PBTTT. The two former subcells are extracted from a structural refinement whereas for C12-PBTTT it was obtained by molecular mechanics calculations.¹³ For all three structures, the alkyl side chains form a different sublattice.⁴³ Following the nomenclature of polymethylene lattices by Kitaigorodski, form I P3HT and PDOPT show an **O**-type sublattice ($a_0=4.96\text{\AA}$, $b_0=4.4\text{\AA}$, $\gamma_0=90^\circ$) whereas PBTTT has an **M**-type sublattice ($a_0=4.2\text{\AA}$, $b_0=4.4\text{\AA}$, $\gamma_0=111^\circ$). For these sublattices, the density of the alkyl side chain (area per stem) follows the progression : PDOPT (20.17\AA^2), PBTTT (24.5\AA^2) and form I P3HT (27\AA^2). As a matter of fact, neither P3HT nor PBTTT did show such high levels of crystallinity as observed here in PDOPT. As an example, Figure S5 shows one of the most well defined ED patterns of an oriented P3HT film crystallized by high-T rubbing at 180°C . The ED pattern of highly oriented and crystalline P3HT always shows fuzzy reflections, indicative of disorder in the side chain packing. The same is true for C12-PBTTT which shows only a few mixed indices reflections in thin films.²² In PDOPT, neither streaking, nor fuzzy reflections, two common signatures of structural disorder,

are observed in the epitaxied films. This comparison points at a highly ordered *n*-octyl side chain sublattice in PDOPT compared to loose and defective side chain packing of non interdigitated *n*-hexyl side chains in form I P3HT.¹⁵ The comparison between the three polymers suggests that the overall crystallinity of the CPs is correlated, at least in part, to the density of the side chain sublattice: the higher the density of side chain packing, the larger the overall crystallinity of the CP.

In regular polymethylene sublattices, well defined offsets along the polymethylene chain direction are observed.⁴³ The analysis of the three refined polythiophenes indicates that the grafted extremity of the side chains to the polythiophene backbone imposes a sterical limit that impedes the alkyl side chains to adopt the most favorable packing along their long axis. In other words, the polymethylene sublattice might be optimized with respect to the packing of the chains in the plane perpendicular to the polymethylene chain direction, but not in the direction parallel to it.

The results on PDOPT further suggest that planarization of conjugated backbones can be enforced in systems in which π - π stacking is absent, provided that the alkyl side chains can form a dense sublattice. The phenyl unit between the solubilizing alkyl chains and the conjugated backbone is particularly beneficial because it helps reducing the direct impact of the packing constraints imposed by the ordering of the alkyl side chains on the polythiophene backbone conformation, a prevailing situation observed in poly(alkylthiophene)s such as P3HT and C₁₂-PBTTT for which the alkyl side chains are directly linked to the conjugated backbone. In addition, in the case of P3HT, regioregularity defects impeded a tight packing of side chains and can therefore rupture chain conjugation by twisting of the backbone. More generally, packing defects of the side chains can cause unwanted twisting of the backbone, shortening conjugation

lengths and reducing intra-chain transport. It can be anticipated that the ordering in phenyl substituted polythiophenes might be further improved by the use of symmetric 3,5-dialkylphenyls.

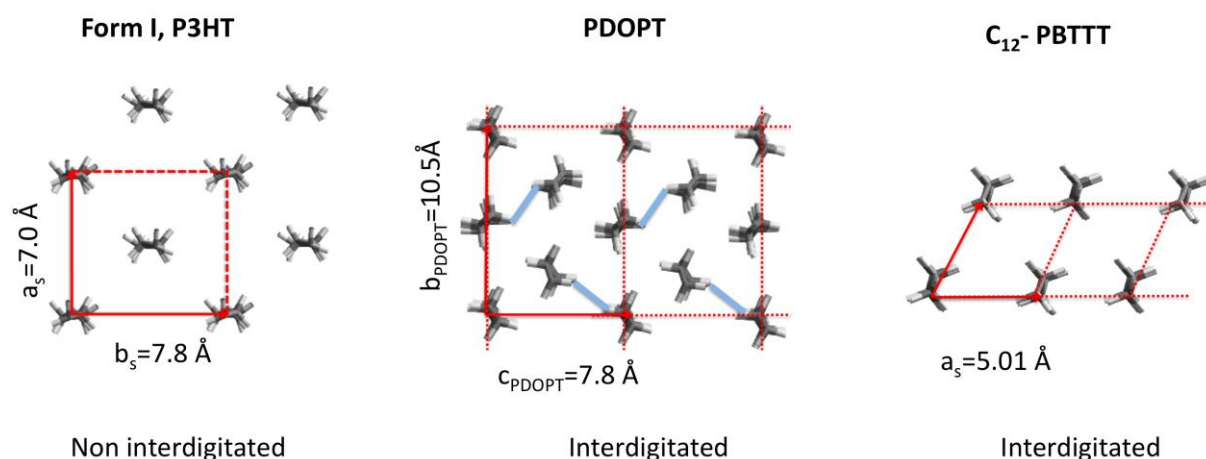


Figure 10. Comparison of the packing of *n*-alkyl side chains in polythiophene semiconductors : form I P3HT,¹⁵ PDOPT and C12-PBTTT. The structure of C12-PBTTT is described in reference 13. The views show the subcells formed by alkyl side chains when viewed along their long axis. For PDOPT, the phenyls linking *n*-octyl side chains are sketched as light blue segments.

V. Conclusion

Epitaxy of a phenyl-substituted polythiophene in which π - π interactions are absent on naphthalene leads to remarkable orientation and crystallinity in thin films with single-crystal-like diffraction patterns. As a consequence, absorption and photoluminescence are highly anisotropic. PDOPT films show a periodic lamellar morphology typical of semi-crystalline polymers. A transition from extended to folded chain crystallization is observed with increasing M_n (transition occurs at $M_n \sim 13$ kDa). Similarly to P3HT, the lamellar period scales first with DP_n and saturates at 28-29 nm in both polymers. This

behaviour is therefore characteristic of the polythiophene folding, irrespective of the chemical structure of the side chains. A Gibbs-Thomson analysis yielded $T_m^0=127.6^\circ\text{C}\pm 1^\circ\text{C}$ from melting temperatures determined by DSC and lamellar periods L measured by TEM. Single-crystal like electron diffraction patterns corresponding to different crystal orientations help establish the structure of PDOPT. Despite the absence of π - π stacking, PDOPT chains are perfectly planarized and the side chains form a dense and highly ordered sublattice. The comparison between P3HT (form I), C12-PBTTT and PDOPT suggests that the overall crystallinity of the CPs is correlated, at least in part, to the density of the side chain sublattice. It will be of high interest to evaluate the effect of the absence of π -stacking in PDOPT on the overall charge transport in comparison to π -stacking polythiophenes such as P3HT i.e. compare PDOPT with dominant 1D intra-chain charge transport and P3HT where both intra-chain and inter-chain charge transport coexist.

Acknowledgments

Support from the DFG (IRTG 1642 and project SO 1213/5-1) is gratefully acknowledged. M.B. acknowledges also the support from the interreg IV-A Rhin Solar program (project C25). B. Lotz is acknowledged for fruitful discussions. M. Schmutz and C. Blanck are acknowledged for technical support in TEM. We are grateful to Patrick Brocorens for supplying the structural model of C12-PBTTT used in the comparative study of this work.

References

- (1) Holliday, S. ; Donaghey, J. E. and McCullough, I. Advances in Charge Carrier Mobilities of Semiconducting Polymers Used in Organic Transistors. *Chem. Mater.* **2014**, 26, 647- 663.
- (2) H. Klauk in Organic electronics : Materials, manufacturing and applications, Wiley, 2006, p. 1
- (3) Biniek, L. ; Fall, S. ; Chochos, C. L. ; Anokhin, D. V. ; Ivanov, D. A. ; Lecerc, N. ; Leveque, P. and Heiser, T. Impact of the Alkyl Side Chains on the Optoelectronic Properties of a Series of Photovoltaic Low-Band-Gap Copolymers. *Macromolecules* **2010**, 43, 9779 – 9786.
- (4) Aasmundveit, K. E.; Samuelsen, E. J.; Mammo, W.; Svensson, M.; Andersson, M. R.; Petterson, L. A. A. and Inganäs, O. Structural Ordering in Phenyl-Substituted Polythiophenes. *Macromolecules* **2000**, 33, 5481 – 5489.
- (5) Yiu, A. T. ; Beaujuge, P. M. ; Lee, O. P. ; Woo, C. H. ; Toney, M. F. and Fréchet, J. M. J. Side-Chain Tunability of Furan-Containing Low-Band-Gap Polymers Provides Control of Structural Order in Efficient Solar Cells. *J. Am. Chem. Soc.* **2012**, 134, 2180 – 2185.
- (6) Kline, R. J. ; Delongchamp, D. M. ; Fischer, D. A. ; Lin, E. K. ; Richter, L. J. ; Chabynyc, M. L. ; Toney, M. F. ; Heeney, M. and McCulloch, I. Critical Role of Side-Chain Attachment Density on the Order and Device Performance of Polythiophenes. *Macromolecules* **2007**, 40, 7960-7965.
- (7) Lee, J. ; Han, A.-R. ; Yu, H. ; Shin, T. J. ; Yang, C. and Oh, J. H. Boosting the Ambipolar Performance of Solution-Processable Polymer Semiconductors via Hybrid Side-Chain Engineering. *J. Am. Chem. Soc.* **2013**, 135, 9540 – 9547.
- (8) Kang, I. ; Yun, H.-J. ; Chung, D. S. ; Kwon, S.-K. and Kim, Y.-H. Record High Hole Mobility in Polymer Semiconductors via Side-Chain Engineering. *J. Am. Chem. Soc.* **2013**, 135, 14896 – 14899.
- (9) Pandey, S. S. ; Takashima, W. ; Nagamatsu, S. ; Endo, T. ; Rikukawa, M. ; Kaneta, K. Regioregularity vs regiodandomness : effect on photocarrier transport in poly(3-hexylthiophene). *Jap. J. Appl. Phys.* **2000**, 39, L94.
- (10) Roux, C. and Leclerc, M. Thermochromic Properties of Polythiophene Derivatives: Formation of Localized and Delocalized Conformational Defects. *Chem. Mater.* **1994**, 6, 620-624.

- (11) Noriega, R.; Rivnay, J.; Vandewal, K.; Koch, F. P. V.; Stingelin, N.; Smith, P.; Toney, M. F. and Salleo, A. A general relationship between disorder, aggregation and charge transport in conjugated polymers. *Nat. Mater* **2013**, *12*, 1038.
- (12) Rahimi, K. ; Botiz, I. ; Stingelin, N. ; Kayunkid, N. ; Sommer, M. ; Koch, F. ; Nguyen, H. ; Coulembier, O. ; Dubois, P. ; Brinkmann, M. and Reiter, G. Controllable Processes for Generating Large Single Crystals of Poly(3-hexylthiophene). *Angew. Chem. Int. Ed.* **2012**, *51*, 11131.
- (13) Cho, E. ; Risko, C. ; Kim, D. ; Gysel, R. ; Miller, N. C. ; Breiby, D. W. ; McGehee, M. D. ; Toney, M. F. ; Kline, R. J. and Brédas, J.-L. Three-Dimensional Packing Structure and Electronic Properties of Biaxially Oriented Poly(2,5-bis(3-alkylthiophene-2-yl)thieno[3,2-*b*]thiophene) Films. *J. Am. Chem. Soc.* **2012**, *134*, 6177.
- (14) Bueno, A.; Nguyen, H. S.; Raos; G.; Gila, L.; Cominetti, A.; Castellani, M. and Meille, S. V. Form II Poly(3-butylthiophene): Crystal Structure and Preferred Orientation in Spherulitic Thin Films. *Macromolecules* **2010**, *43*, 6772.
- (15) Kayunkid, N. ; Uttiya, S. and Brinkmann, M. Structural Model of Regioregular Poly(3-hexylthiophene) Obtained by Electron Diffraction Analysis. *Macromolecules* **2010**, *43*, 4961.
- (16) Himmerberger, S. ; Duong, D. T. ; Northrup, J. E. ; Rivnay, J. ; Koch, F. P. V. ; Beckingham, B. S. ; Stingelin, N. ; Segalman, R. A. ; Mannsfeld, S. C. B. and Salleo, A. Role of Side-Chain Branching on Thin-Film Structure and Electronic Properties of Polythiophenes. *Adv. Funct. Mater.* **2015**, *2*, 2616 – 2624.
- (17) Brinkmann, M. and Wittmann, J.-C. Orientation of Regioregular Poly(3-hexylthiophene) by Directional Solidification: A Simple Method to Reveal the Semicrystalline Structure of a Conjugated Polymer. *Adv. Mat.* **2006**, *18*, 860.
- (18) Brinkmann, M. and Rannou, P. Effect of Molecular Weight on the Structure and Morphology of Oriented Thin Films of Regioregular Poly(3-hexylthiophene) Grown by Directional Epitaxial Solidification. *Adv. Funct. Mat.* **2007**, *17*, 101.
- (19) a) Nagamatsu, S.; Takashima, W.; Kaneto, K.; Yoshida, Y.; Tanigaki, N. and Yase, K. Polymer field-effect transistors by a drawing method. *Appl. Phys. Lett.* **2004**, *84*, 4608. b) Nagamatsu, S.; Takashima, W.; Kaneto, K.; Yoshida, Y.; Tanigaki, N.; Yase, K. and Omote, K. Backbone Arrangement in “Friction-Transferred” Regioregular Poly(3-alkylthiophene)s. *Macromolecules* **2003**, *36*, 5252. c) Masaki, M.; Ueda, Y.; Nagamatsu, S.; Chikamatsu, M.;

- Yoshida, Y.; Tanigaki, N. and Yase, K. Highly polarized polymer light-emitting diodes utilizing friction-transferred poly(9,9-dioctylfluorene) thin films. *Appl. Phys. Lett.* **2005**, *87*, 243503.
- (20) Crossland, E. J. W.; Tremel, K.; Fischer, F.; Rahimi, K.; Reiter, G.; Steiner, U. and Ludwigs, S. Anisotropic Charge Transport in Spherulitic Poly(3-hexylthiophene) Films. *Adv. Mater.* **2012**, *24*, 839.
- (21) Fischer, F. S. U. ; Trefz, D. ; Back, J. ; Kayunkid, N. ; Tornow, B. ; Albrecht, S. ; Yager, K. ; Singh, G. ; Karim, A. ; Neher, D. ; Brinkmann, M. and Ludwigs, S. Highly Crystalline Films of PCPDTBT with Branched Side Chains by Solvent Vapor Crystallization: Influence on Opto-Electronic Properties. *Adv. Mater.*, **2015**, *27*, 1223.
- (22) Biniek, L.; Leclerc, N.; Heiser, T.; Bechara, R. and Brinkmann, M. Large Scale Alignment and Charge Transport Anisotropy of pBTTT Films Oriented by High Temperature Rubbing. *Macromolecules* **2013**, *46*, 4014.
- (23) Biniek, L.; Poujet, S.; Djurado, D.; Gonthier, E.; Tremel, K.; Kayunkid, N.; Zaborova, E. ;Crespo-Monteiro, N.; Boyron, O.; Leclerc, N. ; Ludwigs, S. and Brinkmann, M. High-Temperature Rubbing: A Versatile Method to Align π -Conjugated Polymers without Alignment Substrate. *Macromolecules* **2014**, *47*, 3871.
- (24) Hamidi Sakr, A. ; Biniek, L. ; Fall, S. and Brinkmann, M. Precise Control of Lamellar Thickness in Highly Oriented Regioregular Poly(3-Hexylthiophene) Thin Films Prepared by High-Temperature Rubbing: Correlations with Optical Properties and Charge Transport. *Adv. Funct. Mat.* **2016**, *26*, 408.
- (25) Brinkmann, M. ; Contal, C. ; Kayunkid, N. ; Djurić, T. and Resel, R. Highly Oriented and Nanotextured Films of Regioregular Poly(3-hexylthiophene) Grown by Epitaxy on the Nanostructured Surface of an Aromatic Substrate. *Macromolecules* **2010**, *43*, 7604.
- (26) M. Brinkmann, L. Hartmann, N. Kayunkid, D. Djurado, Understanding the Structure and Crystallization of Regioregular Poly (3-hexylthiophene) from the Perspective of Epitaxy. *Advances in Polymer Science*, **2014**, *265*, 83 – 106.
- (27) M. Brinkmann, Directional Epitaxial Crystallization and Tentative Crystal Structure of Poly(9,9'-di-*n*-octyl-2,7-fluorene). *Macromolecules*, **2007**, *40*, 7532.
- (28) Brinkmann, M. ; Gonthier, E. ; Bogen, S. ; Tremmel, K. ; Ludwigs, S. ; Hufnagel, M. ; Sommer, M. Segregated versus Mixed Interchain Stacking in Highly Oriented Films of Naphthalene Diimide Bithiophene Copolymers. *ACS Nano*, **2012**, *6*, 10319.

- (29) D. Schiefer, T. Wen, Y. Wang, P. Goursot, H. Komber, R. Hanselmann, P. Braunstein, G. Reiter and M. Sommer *ACS Macro letters*, **2014**, 3, 617-621.
- (30) Y. Wang, B. Heck, D. Shiefer, J. O. Agumba, M. Sommer, T. Wen and G. Reiter, *ACS Macro Letters*, **2014**, 3, 881.
- (31) Hartmann, L.; Tremel, K.; Uttiya, S.; Crossland, E.; Kayunkid, N.; Ludwigs, S.; Vergnat C. and Brinkmann, M. *Adv. Funct. Mat.* **2011**, 21, 4047.
- (32) M. Brinkmann and P. Rannou, *Macromolecules* **2009**, 42, 1125.
- (33) T. S. Salammal, E. Mikayelyan, S. Grigorian, U. Pietsch, N. Koenen, U. Scherf, N. Kayunkid and M. Brinkmann, *Macromolecules* **2012**, 45, 5575
- (34) Kayunkid, N.; Uttiya, S. and Brinkmann, M. *Macromolecules* **2010**, 43, 4961.
- (35) Brinkmann, M. *Macromolecules* **2007**, 40, 7532.
- (36) . S. U. Fischer, N. Kayunkid, D. Trefz, S. Ludwigs and M. Brinkmann, *Macromolecules*, **2015**, 48, 3974 – 3982.
- (37) L. Biniek, P.-O. Schwartz, E. Zabrova, B. Heinrich, N. Leclerc, S. Méry, M. Brinkmann, *J. Mater. Chem. C*, **2015**, 3, 3342.
- (38) S. DeHaven, R. Wincheski and S. Albin *Materials* **2014**, 7, 6291.
- (39) Pope, M. In *Electronic processes in organic crystals*; Oxford University Press: Oxford, 1982; p 26
- (40) F. Panzer, M. Sommer, H. Bässler, M. Thelakkat and A. Köhler, *Macromolecules* 2015, 48, 1543.
- (41) Wu, Z. ; Petzold, A. ; Henze, T. ; Thurn-Albrecht, T. ; Lohwasser, R. H. ; Sommer, M. and Thelakkat, M. Temperature and Molecular Weight Dependent Hierarchical Equilibrium Structures in Semiconducting Poly(3-hexylthiophene). *Macromolecules* 2010, 43, 4646.
- (42) S. Z. D. Cheng in “Phase transitions in polymers. The role of metastable states “. Elsevier, Amsterdam, 2008, p. 112.
- (43) Dorset, L. D. in *Crystallography of the polymethylene chain : an inquiry into the structure of waxes*, IUCr Monographs on crystallography n° 17, Oxford University Press, New York, 2005, pp. 19-28. Structure of polymer single crystals, B. Lotz and J.C.
- (44) Wittmann, J. C. and Lotz, B. Epitaxial crystallization of polymers on organic and polymeric substrates. *Prog. Polym. Sci.* **1990**, 15, 909-948.

Supporting informations

Highly oriented and crystalline films of a phenyl-substituted polythiophene prepared by epitaxy : structural model and influence of molecular weight

Amer Hamidi-Sakr¹, Daniel Schiefer², Sangeetha Covindarassou¹, Laure Biniek¹, Michael Sommer^{2,3,4}, Martin Brinkmann¹

(1) Institut Charles Sadron, CNRS – Université de Strasbourg, 23 rue du loess, 67034 Strasbourg, France

(2) : Institut für Makromolekulare Chemie, Universität Freiburg, Stefan-Meier-Straße 31, 79104 Freiburg, Germany

(3) Freiburg Material Research Center, Universität Freiburg, Stefan-Meier-Straße 21, 79104 Freiburg, Germany

(4) Freiburg Institute for Interactive Materials and Bioinspired Technologies, Georges-Köhler-Allee 105, 79110 Freiburg, Germany

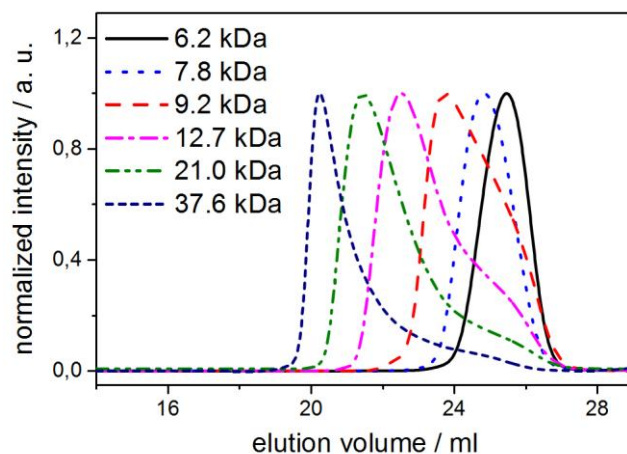


Figure S1. SEC elution profiles of the different PDOPT samples in THF.

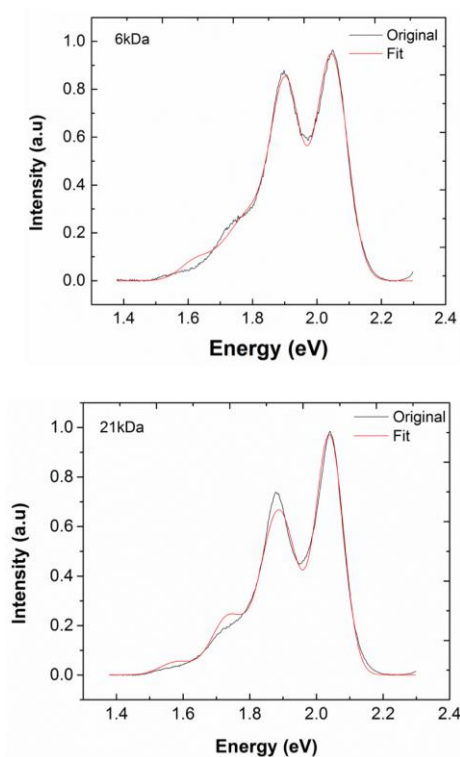


Figure S2. Photoluminescence spectra of oriented PDOPT films prepared by slow-DEC on naphthalene from two different molecular weights (M_n). The figures show the fit of the PL spectra using a simple Frank-Condon progression (in red).

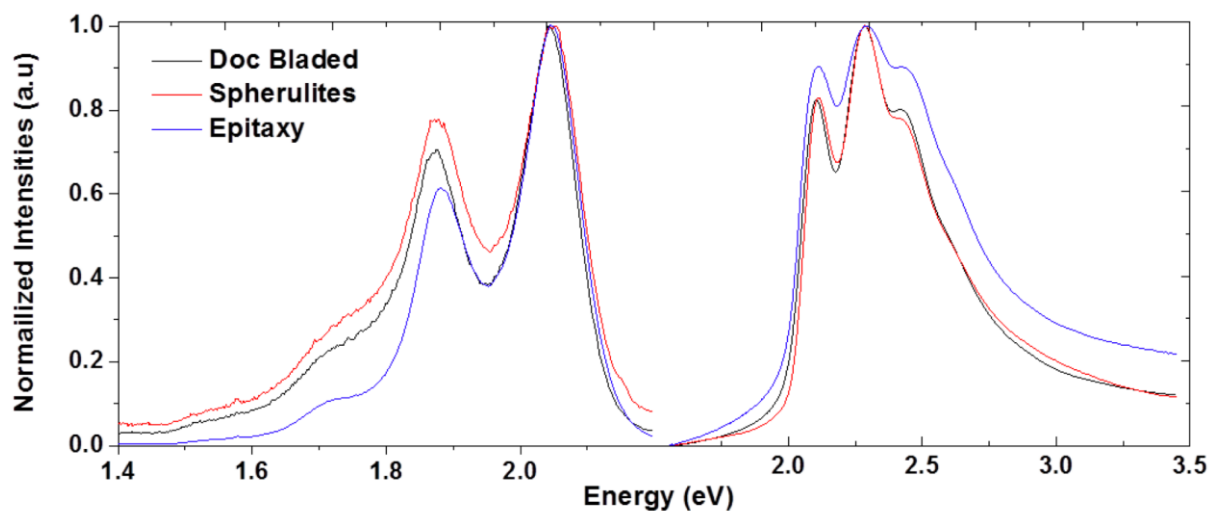


Figure S3. Comparison of the photoluminescence and UV-vis spectra in PDOPT films prepared by doctor blading, isothermal crystallization at 100°C and by slow directional epitaxial crystallization on naphthalene. The PL spectra are normalized with respect to the 0-0 vibronic component whereas the absorption spectra are normalized with respect to the 0-1 component.

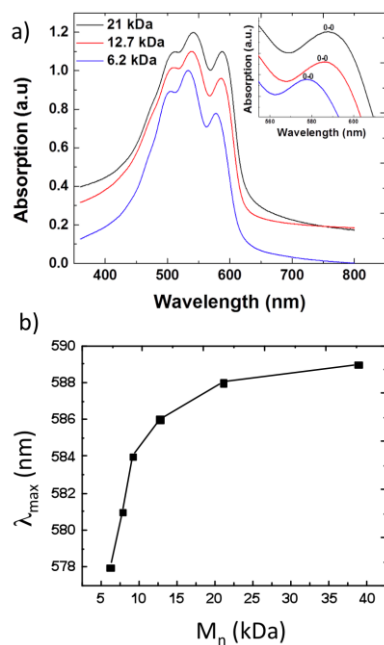


Figure S4. Evolution of optical absorption spectrum of PDOPT films oriented by epitaxy on naphthalene as a function of M_n (incident polarization parallel to the chain direction of PDOPT). The inset shows the shift of the 0-0 transition in the UV-vis absorption spectrum with M_n . b) Evolution of λ_{\max} as a function of M_n .

Figure S4 features the evolution of the UV-vis absorption spectrum and λ_{\max} versus molecular weight of PDOPT. Regarding, the UV-vis absorption, one observes a ~ 10 nm red shift of the 0-0 peak position for the higher M_n of 21 kDa. The position of the 0-0 component in epitaxied P3HT films showed a similar red-shift with increasing M_n .³¹ From the evolution of lamellar period L_p versus M_n , this trend is possibly related to the impact of reduced crystal size along the chain direction on the position of the 0-0 peak position. Higher M_n PDOPT show longer planarized chain segments in the crystalline domains, hence a larger conjugation length which should translate to a red-shift of the 0-0 peak.

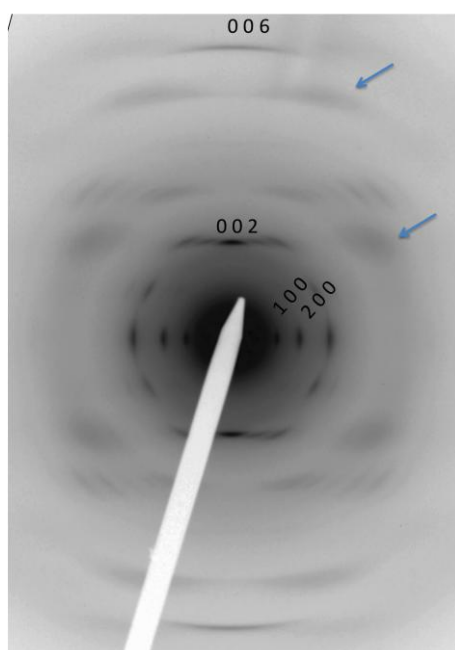


Figure S5. Electron diffraction pattern of a highly crystalline and oriented P3HT film obtained by high-temperature rubbing at 180°C. The two arrows point at fuzzy reflections indicative of structural disorder in the packing of *n*-hexyl side chains in form I P3HT.